Phase Separation and Crystallization Behavior in Extruded Polypropylene/Ethylene–Propylene Rubber Blends

JONG KWAN LEE,[1] JOO HYUNG LEE,[1] KWANG HEE LEE,[1] BYUNG SUK JIN[2]

[1] Center for Advanced Functional Polymers, School of Chemical Science and Engineering, Inha University, Inchon 402-751, Korea

[2] Department of Applied Chemistry, Dongduk Women's University, Seoul 136-714, Korea

Received 3 February 2000; accepted 1 August 2000

ABSTRACT: Liquid–liquid (L–L) phase separation and its effects on crystallization in polypropylene (PP)/ethylene–propylene rubber (EPR) blends obtained by melt extrusion were investigated by time-resolved light scattering (TRLS) and optical microscopy. L–L phase separation via spinodal decomposition (SD) was confirmed by TRLS data. After L–L phase separation at 250°C for various durations, blend samples were subjected to a temperature drop to 130°C for isothermal crystallization, and the effects of L–L phase separation on crystallization were investigated. Memory of the L–L phase separation via SD remained for crystallization. The crystallization rate decreased with increasing L–L phase-separated time at 250°C. Slow crystallization for the long L–L phase-separated time could be ascribed to decreasing chain mobility of PP with a decrease in the EPR component in the PP-rich region. The propylene-rich EPR exhibited good affinity with PP, leading to a slow growth of a concentration fluctuation during annealing. © 2001 John Wiley & Sons, Inc. J Appl Polym Sci 81: 695–700, 2001

Key words: polypropylene; ethylene–propylene rubber; phase separation; crystallization

INTRODUCTION

Polypropylene (PP) homopolymer, although having a number of valuable properties, exhibits poor low-temperature impact resistance. This shortcoming is due to its relatively high glass-transition temperature (T_g). The incorporation of an elastomer as a toughening agent is an effective way to improve the low-temperature impact strength of PP. Various elastomers have been used as impact modifiers, but ethylene–propylene rubber (EPR) is the most common. Extensive research has been carried out by many investigators to understand the characteristics of PP/EPR blends. In particular, considerable progress has been made in elucidating the morphology of EPR, that is, the shape and size distribution of EPR domains, the adhesion at the interface, and the nature and structure of EPR domains.[1]

In PP/EPR blends obtained by melt extrusion, we found that liquid–liquid (L–L) phase separation at high temperatures was very similar to spinodal decomposition (SD), which should originate from a partially miscible system. When the blend has a lower critical solution temperature (LCST) or upper critical solution temperature (UCST) phase diagram, the formation of crystalline structures should be affected by L–L phase

Correspondence to: K. H. Lee (polylee@inha.ac.kr).

Contract grant sponsor: Center for Advanced Functional Polymers; contract grant sponsor: Inha University Foundation.

Journal of Applied Polymer Science, Vol. 81, 695–700 (2001)

separation.[2,3] If the LCST is located above the melting point of PP, L–L phase separation will precede crystallization and have a significant influence on crystallization. To better control the physical properties of the materials, we need more information on phase behavior and its effects on crystallization, and so we investigated the phase separation and crystallization behavior in extruded PP/EPR blends.

We first carried out time-resolved light scattering (TRLS) studies to confirm L–L phase separation via SD in PP/EPR blends, and we investigated the effects of L–L phase separation on crystallization.

EXPERIMENTAL

Materials

Isotactic PP was supplied by LG Chemical Co. (Korea) The density was 0.908 g/cm^3, and the melt flow rate measured by ASTM D1238L was 60. Two commercial EPRs produced by SK Co. (Korea) were used. EPR-1 contained 67 mol % ethylene, and the Mooney viscosity, (ML_{1+4} at 125°C) measured according to ASTM D1646 was 12. EPR-2 (ML_{1+4} at 125°C = 14) contained 54 mol % ethylene.

PP/EPR binary blends were melt-mixed at 250°C on a 30-mm corotating twin-screw extruder (Werner Pfleiderer) at a speed of 200 rpm. The screw configuration was basic kneading blocks, followed by gear mixer flights, to produce a medium shear and a high mixing configuration. In each run, the extrudate was quickly quenched in ice water to freeze the structure in the melt and then was chopped into granules. The composition of the PP/EPR blends was 70/30 w/w.

TRLS and Optical Microscopy (OM)

A thin-film specimen (ca. 15 μm thick) was prepared by blend pellets being pressed between cover glasses at 250°C. Immediately after the melt pressing, the specimen was quickly transferred onto a hot stage in a light scattering photometer equipped with a charge-coupled-device camera,[4] and the kinetics of L–L phase separation were investigated.

After L–L phase separation at 250°C for a certain time, the sample was rapidly transferred onto a light scattering hot stage set at 130°C for isothermal crystallization, and the effects of L–L phase separation on crystallization were investigated. A polarized He–Ne gas laser with a wavelength of 632.8 nm was applied to the film specimen. V_v geometry, in which the optical axis of the analyzer was set parallel to that of the polarizer, was used.

The final morphology of the crystallized specimen at 130°C was observed with OM.

RESULTS AND DISCUSSION

L–L Phase-Separation Behavior

It is well known that different mechanisms are effective during L–L phase separation. Structures with spherical precipitates are indicative of nucleation and growth, and a pattern with two structurally equivalent interpenetrating phases reflects SD. Structure evolution in the early stages of demixing is generally controlled by either of these two mechanisms. Nucleation is the process of generating a large concentration fluctuation, which leads directly to the formation of a nucleus of the new equilibrium phase. After the nucleus has formed, it can increase in size. Growth is accomplished by the regular diffusion of the chains. However, SD implies a continuous growth of the amplitude of a concentration, starting from infinitesimal vales and moving to the final state of two equilibrium phases. In SD, the chains diffuse toward higher concentrations; this corresponds formally to a negative diffusion coefficient. The most convenient technique for the verification of phase-separation mechanisms is scattering experiments because they probe the concentration fluctuations directly.

Figure 1 shows a change in one-dimensional V_v scattering profiles with the L–L phase-separation time (t_s), in which the scattering vector $\mathbf{q}$ is defined as $\mathbf{q} = (4\pi/\lambda')\sin(\theta/2)$, where λ' is the wavelength of light in the specimen and θ is the scattering angle. Even at $t_s = 0$, a weak scattering peak appears at large $\mathbf{q}$, suggesting an appreciable development of L–L phase separation in the quenched and remelt specimens. The peak intensity (I_m) increases with t_s, and its position shifts to smaller angles, implying that the L–L phase separation proceeds via an SD mechanism.

The phase-separation process seen in Figure 1 can be interpreted by the power–law relationship. This problem was discussed by Langer et al.[5] on the basis of nonlinear statistical consideration.

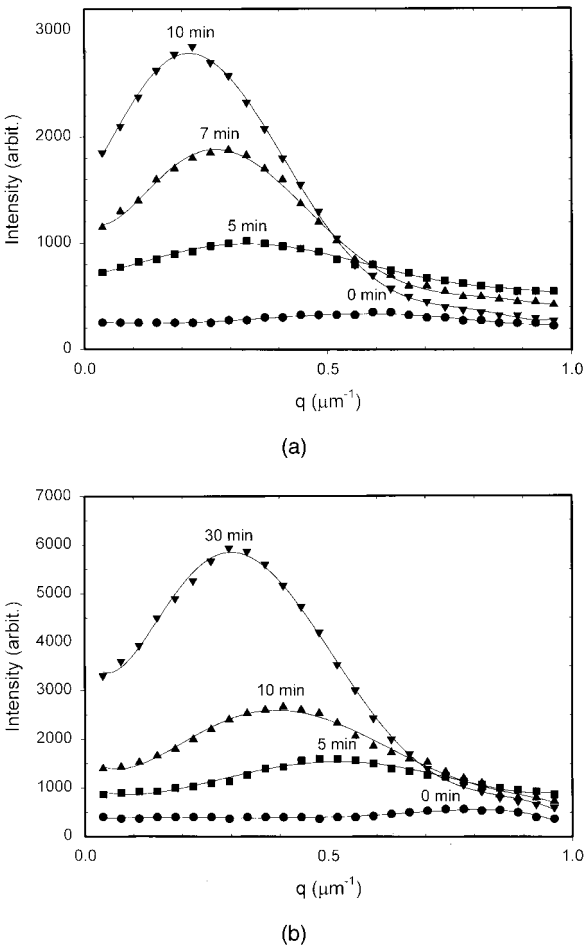

Figure 1 Changes in the light scattering profiles of PP/EPR blends during L–L phase separation at 250°C: (a) PP/EPR-1 blend and (b) PP/EPR-2 blend.

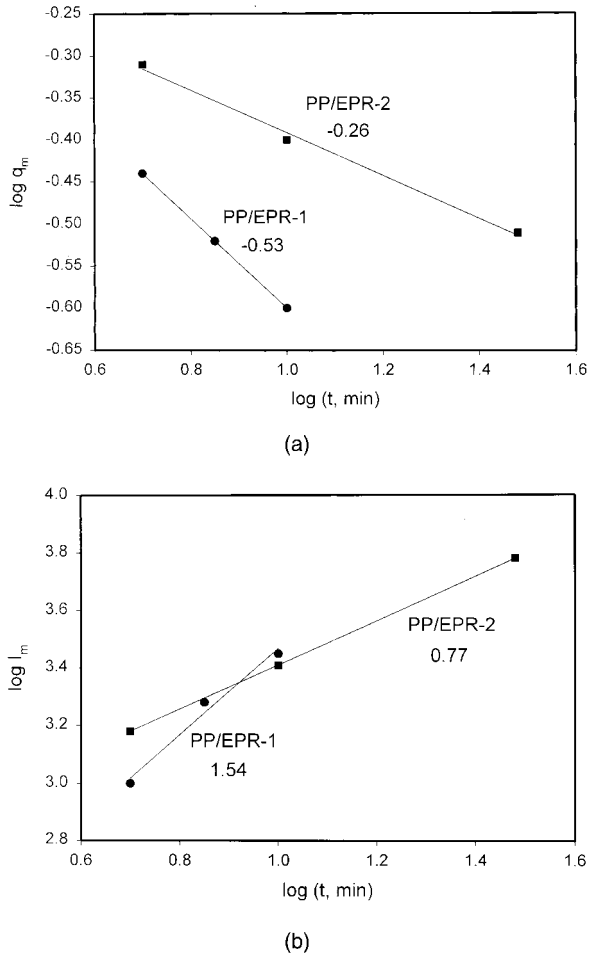

Figure 2 Log–log plots of (a) $\mathbf{q}_m(t) \propto t^{-\alpha}$ and (b) $I_m(t) \propto t^{\beta}$.

The theory predicts a power–law scheme for the intermediate to late stages of SD:

$$\mathbf{q}_m(t) \propto t^{-\alpha} \tag{1}$$

$$I_m(t) \propto t^{\beta} \tag{2}$$

where α and β are the critical exponents. Figure 2(a,b) shows the log–log plots of $\mathbf{q}_m$ and I_m versus t_s, respectively. The β/α ratio is approximately 3, which is in good agreement with the dynamics of cluster coalescence, as suggested by Binder and Stauffer[6] for the late stage of SD or by Siggia[7] for the intermediate stage.

In Figure 3, the periodic length (Λ_m) obtained by the application of the Bragg equation to the peak position of the light scattering profiles is plotted as a function of t_s. An increase in Λ_m with t_s can be clearly seen. Λ_m of the PP/EPR-2 system is smaller than that of the PP/EPR-1 system, suggesting the slower growth of SD. The propylene-rich EPR (EPR-2) may exhibit better solubility

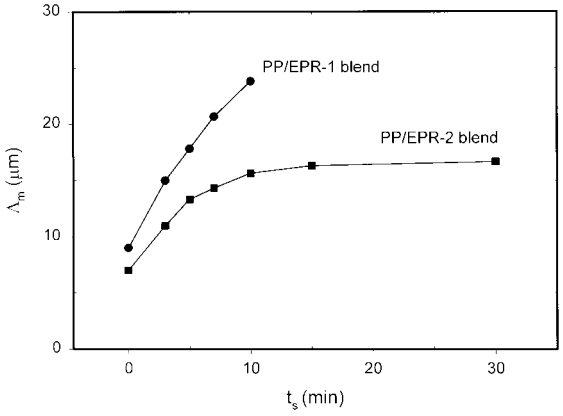

Figure 3 Change in Λ_m with t_s.

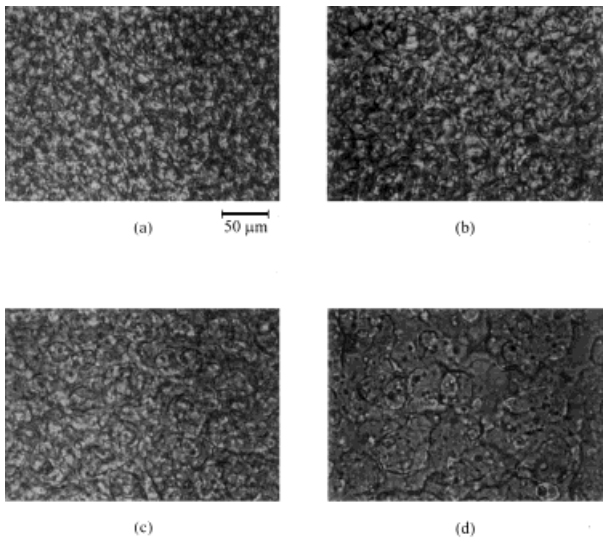

Figure 4 Optical micrographs of the PP/EPR-1 blend crystallized at 130°C for 10 min after the L–L phase separation at 250°C for t_s = (a) 0, (b) 5, (c) 10, and (d) 30 min.

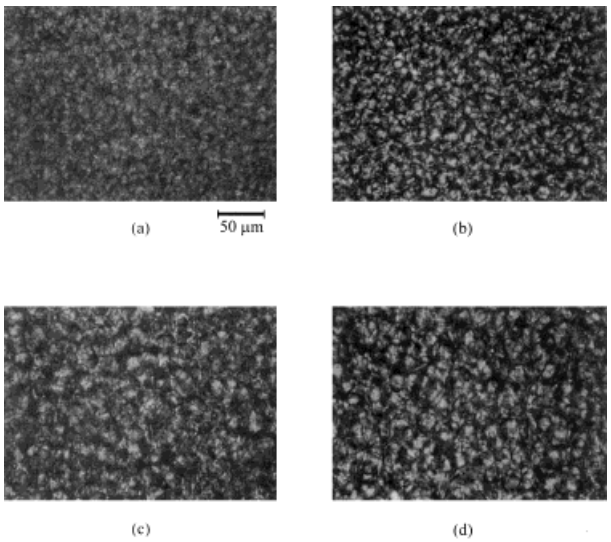

Figure 5 Optical micrographs of the PP/EPR-2 blend crystallized at 130°C for 10 min after the L–L phase separation at 250°C for t_s = (a) 0, (b) 5, (c) 10, and (d) 30 min.

with PP at high shear fields, leading to a slower L–L demixing in the quiescent state.

Supplemental evidence for L–L phase separation was provided through observations of structure formation at 130°C. The apparent mutual diffusion coefficient (D_{app}) at 130°C is very low.[8] This implies that the L–L phase-separation rate may be negligible at 130°C. The crystallization rate of PP is very high (crystallization was completed in about 10 s, as shown later in Fig. 8). In such a case, the L–L phase-separation morphology, that is, the periodic and interconnected structure, could be preserved during crystallization.[2] Figures 4 and 5 show optical micrographs of the PP/EPR blends crystallized at 130°C after L–L phase separation at 250°C. A significant change in the morphology of the blends with annealing at 250°C is observed. In the beginning [Figs. 4(a) and 5(a)], it is not clear which phase is continuous and which is dispersed. At the later stage of L–L phase separation, phase connectivity grows and eventually breaks up into a macroscopic spherical texture. These are characteristic of the SD mechanism. The spacing between dark and bright regions in micrographs was in good agreement with Λ_m obtained from the light scattering profiles.

On the basis of these results, a scenario of the melt extrusion to yield near a homogeneous blend may be given as follows. At high shear rates in the extruder, the spinodal temperature (T_s) in the LCST phase diagram may be elevated, as shown by the arrow in Figure 6, and one phase region becomes wider.[9–12] Thus, the system undergoes phase dissolution. The dissolution continues until a new composition is reached in the mixture. The compositions X_A and X_B at a static condition move to the compositions X_A' and X_B' in the shear field. This could be the case for these PP/EPR blends. If T_s in the shear field is raised above the barrel

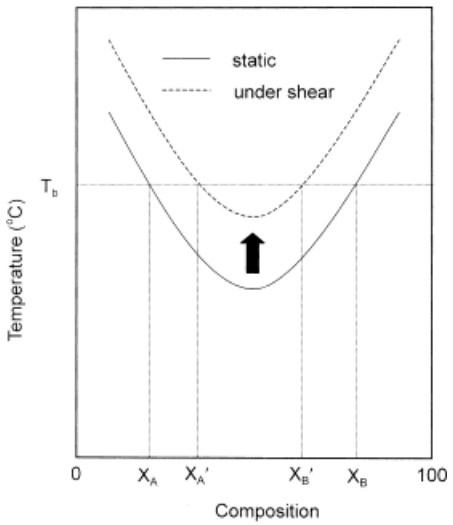

Figure 6 Schematic drawing of changes in the phase diagram with the shear rate. The arrow indicates T_s elevated at a high shear rate.

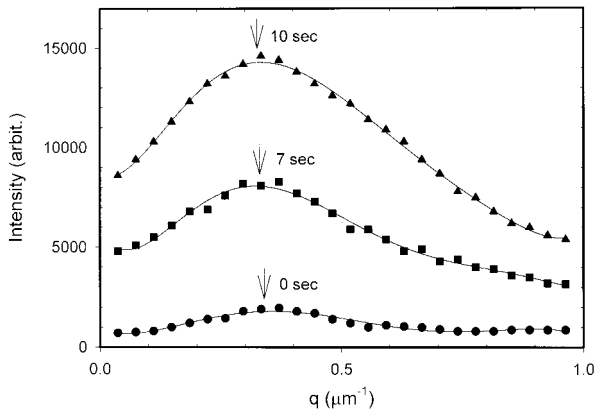

Figure 7 Changes in the light scattering profiles of the PP/EPR-1 blend during crystallization at 130°C after t_s = 5 min.

temperature (T_b), the mixing can be done in the one-phase region to obtain a homogeneous mixture. The phase diagram in Figure 6 is just a schematic illustration and does not have any quantitative significance; it indicates that the mixture is thermodynamically unstable. It is conceivable that the blend may not have an LCST phase diagram but rather has an UCST phase diagram. In that case, T_s in the shear fields should be lowered to induce the dissolution of the components. Once the melt is extruded from the nozzle, the shear rate becomes 0 and T_s immediately falls to a static value, so SD proceeds until the structure is fixed by crystallization.

Effects of L–L Phase Separation on Crystallization

L–L phase-separated specimens at 250°C for various times were allowed to crystallize with a rapid temperature drop to 130°C for isothermal crystallization. Figure 7 shows a typical change in the V_v scattering profiles during crystallization at 130°C. The peak position, indicative of Λ_m caused by SD at 250°C, is kept constant, and I_m increases with time. A constant Λ_m value suggests that L–L phase separation no longer proceeds during crystallization. The increase in I_m should be caused by crystallization. The crystallization increases the refractive index of the PP-rich region, resulting in a larger optical contrast in the phase-separated system.

To discuss crystallization, we can use the light scattering invariant in the V_v mode, Q_{V_v}. The time variation of Q_{V_v} is shown in Figure 8. Q_{V_v} is kept constant for a while, increases rapidly, and attains a maximum value. Then, Q_{V_v} decreases slightly and levels off. A finite value of Q_{V_v} at time 0 may be ascribed to the density fluctuation formed by SD at 250°C before crystallization onset. Constant Q_{V_v} at an early time is indicative of the incubation period typical of the nucleation process of the crystallization. The rapid increase of Q_{V_v} should be ascribed to PP crystallization. The slight decrease and leveling off of Q_{V_v} suggest that PP in the EPR-rich region may crystallize slowly at the later stage, reducing differences in the refractive index between the separated regions.

Neglecting the small contribution from optical anisotropy, we can approximate Q_{V_v} of crystallized polymer systems:[13]

$$Q_{V_v} \propto \phi_c(1 - \phi_c)(\alpha_c - \alpha_0) \tag{3}$$

where ϕ_c is the volume fraction of crystalline aggregate and α_c and α_0 are the polarizabilities of

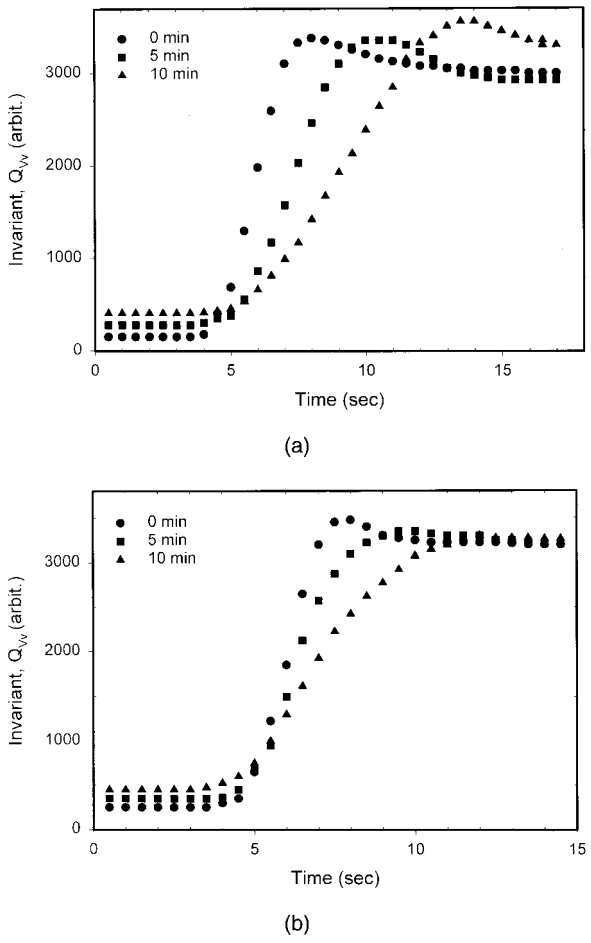

Figure 8 Time variation of the invariant Q_{V_v} in PP/EPR blends crystallized at 130°C after L–L phase separation at 250°C for t_s = 0, 5, and 10 min: (a) PP/EPR-1 blend and (b) PP/EPR-2 blend.

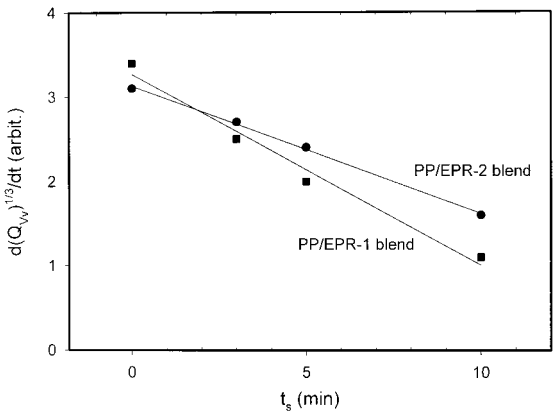

Figure 9 Change in G with t_s.

crystalline aggregate and the melt, respectively. At the early stage of crystallization, eq. (3) is further approximated by

$$Q_{V_v} \propto \phi_c(\alpha_c - \alpha_0) \tag{4}$$

Q_{V_v} is assumed to be proportional to ϕ_c, so that the linear growth rate of crystallite G is

$$G \propto d(Q_{V_v})^{1/3}/dt \tag{5}$$

Therefore, one can estimate G from the initial slope of the time variation of $(Q_{V_v})^{1/3}$. G, estimated by eq. (5), is shown as a function of t_s in Figure 9. G decreases with t_s; G for $t_s = 5$ and 10 min is much smaller than that for $t_s = 0$ min. This may come from differences in the amounts of the EPR component in the PP-rich region. The growth of the concentration fluctuation is realized by uphill diffusion; A molecules diffuse into the A-rich region from the B-rich region. Thus, in PP/EPR blends EPR molecules are forced to move from the PP-rich region to the EPR-rich region. As the L–L phase separation proceeds, the amount of EPR in the PP-rich region should decrease by SD. In the PP-rich region, T_g increases as the amount of EPR decreases. The crystallization rate consists of nucleation and diffusion rates. The higher T_g reduces the diffusion rate so that the crystallization rate may be correspondingly reduced.

Figure 9 shows that the dependence of G on t_s is noticeably influenced by the type of EPR. A stronger influence is observed for the PP/EPR-1 blend. This can be explained by differences in the growth rate of the concentration fluctuation; that is, because the concentration fluctuation by SD occurred more rapidly in the PP/EPR-1 blend, the larger amount of EPR in the PP-rich region decreased with t_s, and the decrease might have retarded crystallization.

CONCLUSIONS

L–L phase separation via SD was found in extruded PP/EPR blends. For the homogeneity of melt-extruded blends, we think that the phase diagram is elevated at high shear rates in the extruder, allowing phase dissolution. The effects of L–L phase separation on the crystalline morphology produced by subsequent crystallization were discussed. Crystallization takes place only in the PP-rich region, so that the memory of SD (the periodic structure) is preserved. The amounts of the EPR component in the PP-rich region formed by SD were strongly related to the crystallization rate. The amount of EPR in the PP-rich region decreased with increasing t_s, and the decrease retarded the crystallization rate. The propylene-rich EPR exhibited good affinity with PP, leading to a slow growth in the concentration fluctuation during annealing.

REFERENCES

1. Baldwin, F. P.; VerStrate, G. Rubber Chem Technol 1972, 45, 709.
2. Inaba, N.; Sato, K.; Suzuki, S.; Hashimoto, T. Macromolecules 1986, 19, 1690.
3. Inaba, N.; Yamada, T.; Suzuki, S.; Hashimoto, T. Macromolecules 1988, 21, 407.
4. Lee, C. H.; Saito, H.; Inoue, T. Macromolecules 1995, 28, 8096.
5. Langer, J. S.; Baron, M.; Miller, H. S. Phys Rev A 1975, 11, 1417.
6. Binder, K.; Stauffer, D. Phys Rev Lett 1974, 33, 1006.
7. Siggia, E. D. Phys Rev A 1979, 20, 595.
8. Im, S. W.; Lee, K. H.; Lee, C. H. Polymer 1999, 40, 2837.
9. Hindawi, I.; Higgins, J. S.; Galambos, A. F.; Weiss, R. A. Macromolecules 1990, 23, 670.
10. Okamoto, M.; Inoue, T. Polymer 1994, 35, 257.
11. Okamoto, M.; Shiomi, K.; Inoue, T. Polymer 1995, 36, 87.
12. Okamoto, M.; Kotaka, T. Polymer 1997, 38, 1357.
13. Koberstain, J. T.; Russel, T. P.; Stein, R. S. J Polym Sci Polym Phys Ed 1979, 17, 1719.